Orbit Determination for a Jupiter Orbiter Tour of the Galilean Satellites

R. K. Russell* and J. Ellis*
Jet Propulsion Laboratory, Pasadena, Calif.

The Jupiter Orbiter Tour mission requires precise spacecraft state estimates relative to the Galilean satellites to achieve scientific objectives and to utilize gravity assist flybys of the satellites. This paper explores the problems of determining satellite relative spacecraft estimates using a combination of Earth based radiometric and on-board optical data. A Jupiter approach trajectory which encounters Ganymede prior to orbital insertion is initially studied. Ganymede relative errors of less than 100 km are attainable, five days prior to insertion, by including optical data during the approach. The second phase of the study determines the relative navigation accuracies for an equatorial orbiter, with a 33.5 day period and periapsis of 4 R_j and apoapsis of 80 R_j. Satellite relative errors for inbound encounters with Callisto, Ganymede, Europa, and Io are estimated using satellite ephemeris information obtained during the approach phase combined with radio and optical data from the orbiter.

Introduction

CURRENT NASA planning envisions an ambitious Jupiter Tour mission which will arrive at the planet in the year, 1984. The objectives of this mission are to broaden our knowledge of the outer solar system and in particular to extend our understanding of the physical processes at work in the Jupiter and Galilean satellite environment. To achieve these goals, precise spacecraft navigation is a fundamental requirement inasmuch as very near encounters with the satellites are necessary both for the planned scientific investigations and to reduce fuel requirements necessary for orbit insertion about the planet. This paper, then, deals with problems of producing precise spacecraft state estimates relative to the Galilean satellites, with the aid of both Earth-based radio and on-board video data.

The paper is divided into three sections, reflecting three areas of study. In the first phase, the state estimation behavior for a Jupiter approach trajectory having a near encounter with Ganymede is explored. The second section defines the general, radio-based orbit determination characteristics as a function of the Jupiter-relative geometry in the orbit phase. The final section details the satellite-relative state estimation behavior obtained with Earth-based radio and on-board video data for a specific trajectory.

I. Approach Phase

The approach trajectory and associated navigation accuracy analysis presented here would be similar to many such prior planetary approach analyses conducted were it not for recent work[1] which has shown the considerable energy benefit derived from a near encounter with one of the Galilean satellites during planetary approach. The nearer the encounter, the greater the savings in energy required to insert the spacecraft into planetary orbit.

Presented as Paper 74-847 at the AIAA Mechanics and Control of Flight Conference, Anaheim, California, August 5-9, 1974; submitted September 26, 1974; revision received February 12, 1975. This paper presents the results of one phase of research carried at the Jet Propulsion Laboratory, California Institute of Technology, under Contract No. NAS 7-100, sponsored by NASA. The authors would like to express their profound gratitude to M.W. Nead and C.E. Hildebrand for their unstinting efforts on the analysis, development, and checkout of the software which was used in this study. Special thanks go to J.F. Dixon for his analysis and programing efforts which allowed a proper treatment of satellite ephemeris errors.

Index categories: Spacecraft Tracking; Navigation, Control and Guidance Theory; Spacecraft Navigation, Guidance, and Flight Path Control Systems.

*Member of the Technical Staff, Mission Analysis Division.

Table 1 Spacecraft and satellite states at closest approach, July 17, 1984

Joviocentric, Earth-equatorial, mean 1950 space-fixed			
Spacecraft state		Ganymede state	
X	-829,711.89	X	-826,960.12
Y	614,895.05	Y	612,838.86
Z	281,477.99	Z	280,537.64
DX	-6.9364391	DX	-6.8836803
DY	-13.976514	DY	-7.5853451
DZ	-5.3011131	DZ	-3.7211937

As a result, satellite-centered state errors are of principal interest. The present trend in mission design appears to favor Ganymede as the satellite to encounter, slightly prior to planetary periapsis, with a nominal closest approach distance of 1000 km above the surface. These conditions coupled with an arrival epoch of July 17, 1984 lead to the satellite and spacecraft states shown in Table 1.

To complete the specification of the Galilean system, the states of Io, Europa, and Callisto are required. Rather than use Samson's theory, it is assumed here that the satellites undergo circular motion in the Jupiter equator plane. Further, for convenience the satellites are phased such that in the ensuing orbital phase of the mission, near encounters with all the Galilean system will occur on the first inbound periapsis approach. This is done not only to reduce the amount of computer work required to analyze four distinct satellite encounters in orbit phase, but to preserve properly, within the constructs of our computational machinery, the information gained about the states of the satellites from the on-board video system used during the approach phase.

With this information in hand, a covariance analysis was performed under the following assumptions:

A. Data

The available data types are: 1) conventional range-rate†; 2) conventional range†; 3) differenced range-rate; 4) differenced range; and 5) optical measurements (lines and pixels) of the four Galilean satellites. Radio and optical data commence 90 days prior to encounter. Optical data terminates 5 days prior to encounter, with radio data being taken all the

†These data types are assumed to be de-weighted from their actual accuracies so as to minimize the effect on filter performance due to unmodeled accelerations.

way in. The Earth-based radio data is assumed taken by three stations; Goldstone, Woomera, and Madrid, according to the data scheme shown in Fig. 1. A full station cycle is repeated every third day so as to minimize computer costs.

B. Data Weights and Frequency

1) Conventional range-rate: 1 pt/min with a Gaussian error having a standard deviation of 100 mm/sec; 2) conventional range: 1 pt/5 hr, standard deviation of 10 km; 3) differenced range-rate: 1 pt/min where stations overlap, standard deviation of 2.8 mm/sec; 4) differenced range: 2/station cycle, standard deviation of 8.5 m; and 5) optical line and pixel measurements: 1 set/4 hr.

The optical errors are treated in a slightly more complex manner than the radio since they are not assumed to be constant. At a large distance from the satellite they are effectively constant with line and pixel errors being approximately 10 μ rad. As the spacecraft-satellite distance decreases, however, the errors become dominated by the center-finding error, which at present in this analysis is treated as a random error equal to 2% of the diameter of the satellite being tracked. It is this error which effectively sets a lower limit on the state accuracies obtainable both for the spacecraft and the satellite. This error model may not necessarily be comprehensive, but provides a reasonable approximation to the total error. Videometric observable errors should eventually be covered in a thorough study taking all factors such as optical distortion, lighting conditions, s/c motion, etc., into account.

C. Estimated Parameters

1) Spacecraft state (6), 2) planet state (6), 3) planet mass (1), 4) 1st satellite state (6), 5) 2nd satellite state (6), and 6) Ganymede mass (1).

D. Consider Parameters

1) Tracking station locations (6) three stations, (spin radius and longitude treated only), 2) Jupiter gravity harmonic, J_2 (1), 3) biases in the optical sensor (2) (line and pixel) and 4) stochastic accelerations (3) acting on the spacecraft due to attitude control jets.

E. A priori Errors in Parameters

1) Spacecraft state:$\sigma_x = 10^6$km, $x \rightarrow y,z$; $\sigma_{\dot{x}} = 1$ km/sec, $\dot{x} \rightarrow \dot{y}, \dot{z}$; 2) planet state:a fully correlated (6x6) covariance matrix on the Brouwer and Clemence Set III elements; position error relative to the Earth is about 400 km; 3) planet GM:1000 km^3/sec^2; 4) satellite GM's:10% of the nominal; 5) satellite state:400 km in each position coordinate, 4 m/sec in each velocity coordinate; 6) station locations:two levels of station location errors have been assumed in the analysis ("tight" and "loose"). These different error levels would reflect the type of commitment of the DSN to supply and maintain effective station location coordinates to the project. "Tight": σ_{r_s} (spin radius) = 1 m; σ_λ(longitude) = 2 m. "Loose": $\sigma_{r_s} = 3$ m; $\sigma_\lambda = 5$ m. In both "tight" and "loose" station location errors, the correlation factor between station longitudes is assumed to be $\rho = 0.9$; 7) Jupiter gravity harmonic, J_2. $\sigma_{J_2} = 4\text{x}10^{-5}$ (see Ref. 2); 8) the bias errors are assumed to be constant with 10 μrad error in line and pixel biases; and 9) Stochastic acceleration error is 10^{-12} km/sec^2 with a correlation time of 5 days (on all 3 axes).

F. Filtering Strategy

The filter is a weighted, least-squares batch processor. The evaluation is performed in a batch-sequential mode (using a 2-day batch size) when stochastic accelerations are treated as consider parameters. Based on these assumptions, an initial analysis was made to assess the effect of stochastic accelerations on filter performance during Ganymede approach. Figure 2 presents these results for radio data only, using "tight" station location assumptions. As is apparent, the inclusion of stochastic accelerations as consider parameters has virtually no effect on the Ganymede-relative state error.

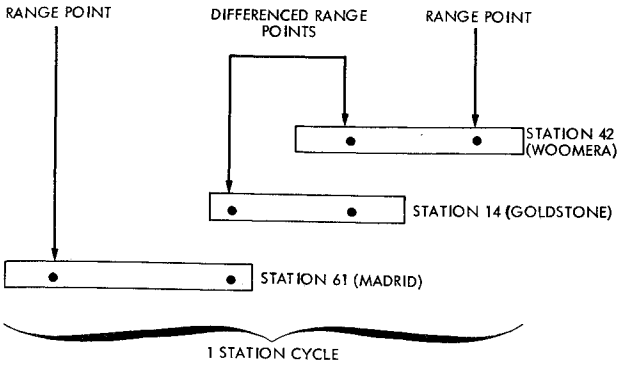

Fig. 1 Radio data scheme.

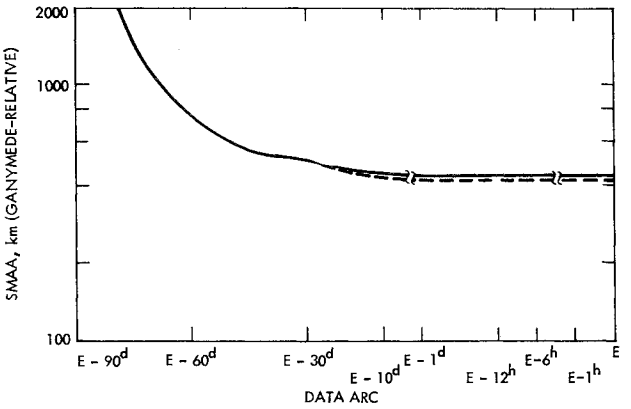

Fig. 2 Ganymede-relative B-plane semimajor axis (SMAA) vs data arc (radio only).

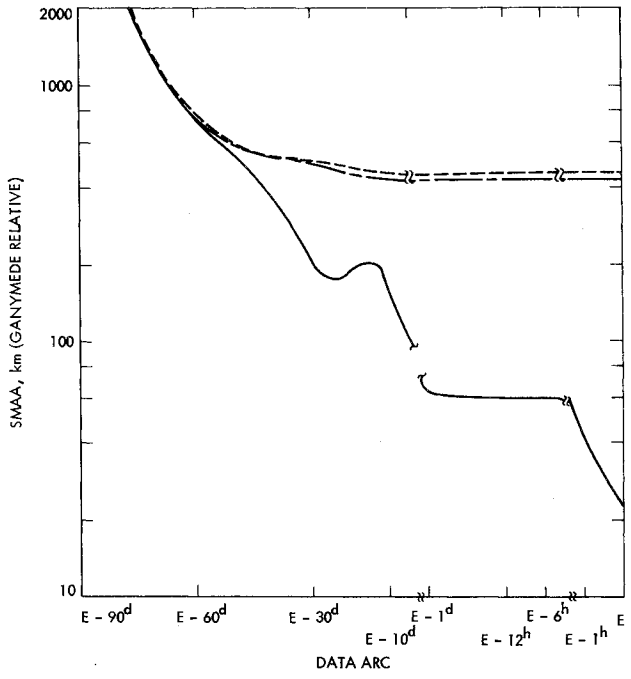

Fig. 3 - - - radio only, "loose" stations, - — - radio only, "tight" stations, —— radio + optical, "loose" stations. Ganymede-relative B-plane semimajor axis (SMAA) vs data arc including radio and optical data.

Thus not only has the state error become limited by the ephemeris errors well in advance of encounter, but the particular combination of radio data types and associated weights has shown itself to be insensitive to unmodeled accelerations acting upon the spacecraft. As a result of this and the insensitivity of optical data to unmodeled accelerations, the lengthy and expensive computer treatment of stochastic

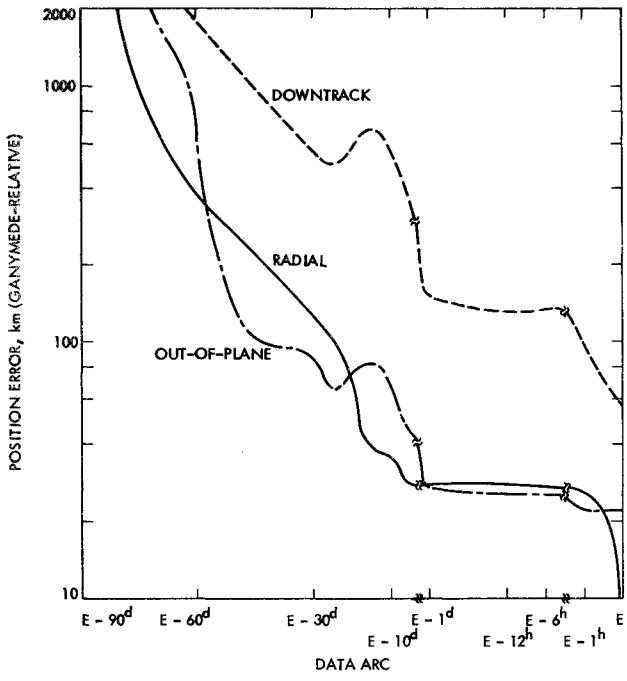

Fig. 4 Ganymede-relative, radial, downtrack, and out-of-plane position errors at encounter vs data arc (radio + optical).

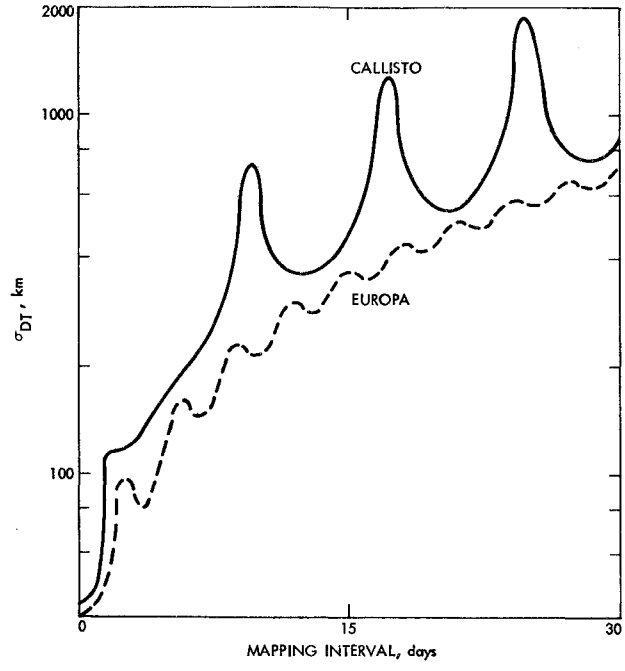

Fig. 5 Mapped downtrack position errors for Callisto and Europa vs mapping interval.

Table 2 Planet-relative satellite position and mean motion errors

Satellite	Position errors at epoch (km) Radial	Down-track	Out-of-plane	Mean motion error (ppm)
Io	21	42	12	14
Europa	23	40	13	16
Ganymede	20	75	15	12
Callisto	35	43	23	14

accelerations will be eliminated for the remaining analysis in the approach phase.

Part of that analysis is displayed in Fig. 3, where on-board optical observations of Ganymede and Callisto are used in conjunction with Earth-based radio tracking to determine not only the spacecraft state, but the states of the observed satellites as well. Shown here is the Ganymede-relative, B-plane semimajor axis as a function of the data arc. When radio data alone is used, the state errors are limited by the satellite ephemeris errors for both the "loose" and "tight" station location error assumptions. The inclusion of optical data, however, brings about a marked improvement in the estimation. It appears that B-plane errors of 60-100 km are achievable from one to five days prior to encounter. It should be mentioned that the bulk of the error in the state is due to the optical biases, whereas J_2 and station locations have virtually no effect.

The local maximum, being manifested by a data arc extending to E-15^d is at present not fully understood. It is known, however, that it is brought about by an increased sensitivity to the optical bias errors which are treated as consider parameters. The general nature of the geometric influence producing this effect has eluded our understanding despite persistent efforts.

Figure 4 displays a breakdown of the state errors at encounter into Ganymede-relative, radial, downtrack, and out-of-plane position errors. By this decomposition it is observed that the principal position error is in the downtrack direction, which of course is linearly related to the time-of-flight error by the Ganymede-relative spacecraft velocity. Here again the local maximum is seen at E-15d.

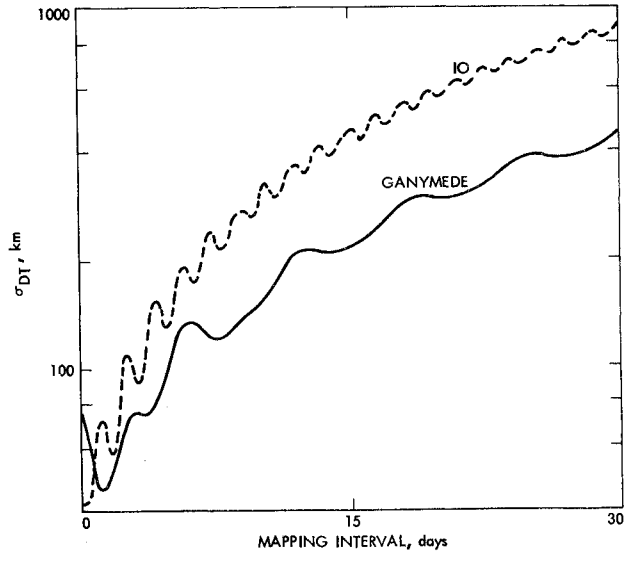

Fig. 6 Mapped downtrack position errors for Io and Ganymede vs mapping intervals.

An area of concern, which has not yet been discussed, but which will become of central importance in the orbit phase, is the nature of the ephemeris errors of the Galilean satellites obtained with on-board optical observations. Table 2 displays a decomposition of the satellite position errors along with the approximate mean motion errors (expressed in parts/million).

The position errors shown here reveal on-board optical data to be a powerful tool with which to determine planet-relative satellite positions. The ability of this data type, by itself, to resolve mean motion, however, is none too good in relation to present knowledge. An illustration of this is provided in Figs. 5 and 6, which display the downtrack‡ errors of these satellites when mapped 30 days (about one orbit period for the satellite orbit examined in Sec. III).

The growth in the downtrack position errors of the satellites is plainly unacceptable. What is necessary is some mechanism to preserve the Earth-based, mean motion knowledge gleaned

‡Radial and out-of-plane errors not displayed as they appear to suffer no growth.

from decades of observation as opposed to relying upon the on-board optical sensor to generate it. The mechanism we have chosen is to construct a fully correlated (7×7) apriori covariance matrix of the errors in the planet-relative satellite state and the central body mass, which has incorporated into it a very tight constraint on the mean motion error.§ This method does indeed preserve the size of the satellite state errors at virtually their initial values for mapping intervals of 30 days when the mean motion error is constrained to 1 part in 10^9.

II. Orbit Phase—General Analysis

The second phase of the study evaluates the influence of the spacecraft orbital geometry on the orbit determination characteristics from Earth based radio data. Factors such as periapsis location, data processing strategies, and effects of unmodeled error sources are explored in a general qualitative sense. The class of orbits is restricted to 33-1/2 day period Jupiter equatorial orbits, in which the periapsis radius is $4\,R_J$ and apoapsis radius is $80\,R_J$. The orbital parameters for this reference family are semi-major axis, 2.997624 x 10^6 km; eccentricity, 0.9047619048, time of periapsis passage, 0 sec.; node, and inclination, both 0°. The argument of periapsis is varied from 0-360°. Such an orbit ensures the possibility of multiple satellite encounters with Io, Europa, Ganymede, and Callisto at 4.5, 9.5, 18.5, and 41 hr before or after Joviocentric periapsis passage. Figure 7 illustrates a typical example of the satellite encounters for this orbit.

A minimum variance batch filter was used to estimate the spacecraft state by processing range rate data from 3 tracking stations. The effects of unmodeled errors in the mass of Jupiter, the zonal gravitational harmonic J_2 and the Earth station locations are considered at the following error levels: GM, 1000 km^3/sec^2; J_2, 0.14 x 10^{-3}; station spin, 3 m and station longitude 5 m. Range rate data is weighted at 1.0 mm/sec.

Figure 8 displays the variation of the Joviocentric spacecraft position error at periapsis as a function of the argument of periapsis. Two data arcs are presented; a full 33 1/2 day orbit of data, and a data span which excludes the data within two days of periapsis.

It is observed for a full revolution of data that when station locations are not considered, there exists a strong sensitivity of the state errors to the argument of periapsis, with extremals occurring when the orbit is in such an orientation that the velocity vector of the spacecraft at periapsis is roughly along the line-of-sight from Earth. For these cases, the deletion of near periapsis data, has the effect of changing maxima to minima. This is because the velocity of the spacecraft is more corrupted at periapsis by the unmodeled forces arising from errors in mass and J_2, and that the deletion of data from that portion of the orbit has the most pronounced effect on filter estimates when the geometry is such that the corrupted velocity at periapsis is most visible in the data (i.e., range-rate radio data). (Thus, for this filter configuration, not only does a strong sensitivity to geometry exist, but to data span as well.) The presence of station location errors, however, when a "near" optimal data span is used, appears to greatly lessen the effect of geometry on state estimation, which in a certain sense is a pleasing result, inasmuch as the ability to alter the argument of periapsis to any great degree for the purpose of reducing orbit determination errors is well out of our control due to energy constraints.

III. Orbit Phase—Mission Specific Analysis

It is the purpose of this section to apply the general and specific information obtained in Secs. I and II to a mission specific trajectory and detail the nature and size of the satellite-relative errors for near encounter with the Galilean satellites. Due to complexity the only encounters treated are inbound (i.e., those encounters prior to Jupiter periapsis passage).

§The design of this covariance matrix is attributed to J.F. Dixon.

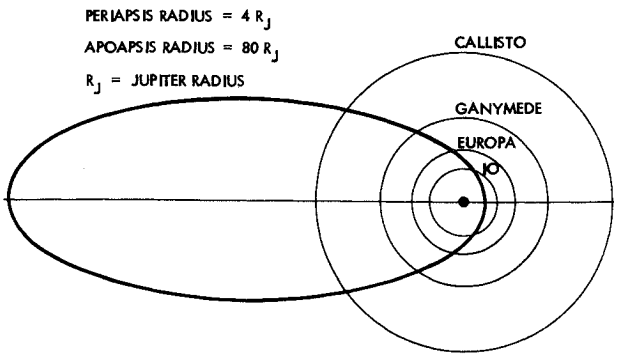

Fig. 7 Jupiter orbiter trajectory.

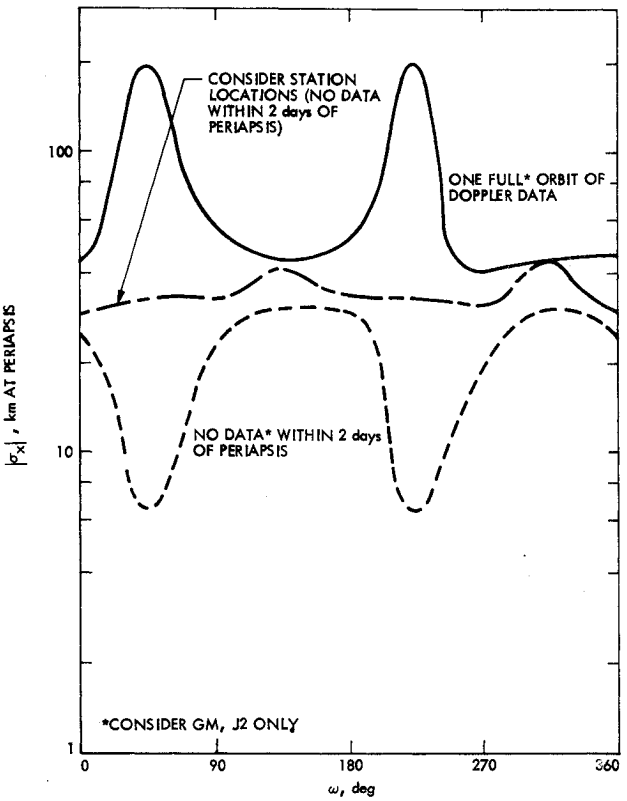

Fig. 8 Position error at periapsis, $|\sigma_x|$, vs argument of periapsis, ω.

Table 3 Classical elements of Jupiter-centered orbit

Classical element	Value
a, semimajor axis	2.997624×10^6 km
e, eccentricity	0.9047619048
T_p, time of periapsis	0^s
Ω, longitude of ascending node[a]	47°
ω, argument of periapsis[a]	0°
i, inclination[a]	0°
P, period	$33^d\ 12^h\ 42^m\ 50^s$

[a] Relative to Jupiter equator.

The trajectory under consideration here is the same in all respects as that in the previous section ($r_p = 4\,R_J$, $r_a = 80\,R_J$) except that the nodal angle relative to the Jupiter vernal equinox is 47°. Table 3 lists the classical element specifications of the orbit.

The assumptions embodied in this phase are the same as those in Sec. I with the following exceptions: 1) of the radio data types available, only conventional range-rate is used. It is assumed to be taken at 1 pt/min with a proper weighting of 1 mm/sec. The radio data arc commences 2^d after periapsis passage; 2) the tracking station data cycle is repeated every

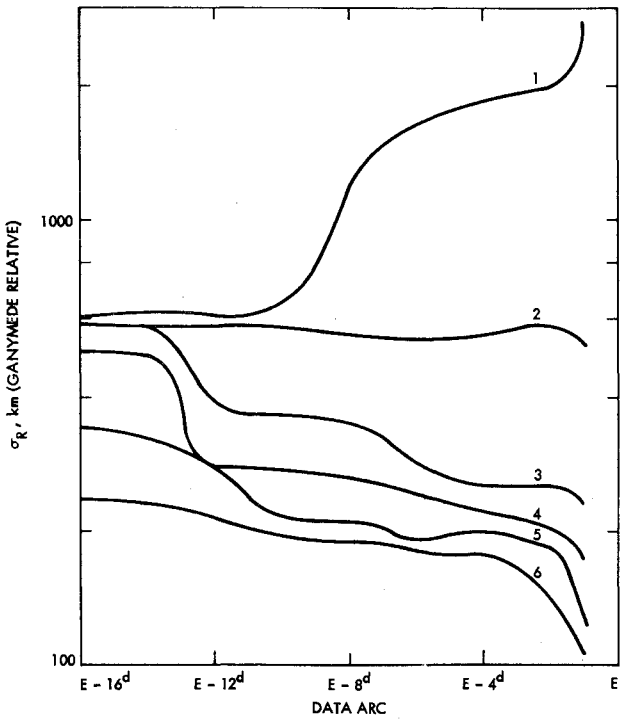

Fig. 9 1) Consider Stochastic accelerations, "loose" stations, radio only, $\tilde{\Gamma}_{sat}$. 2) Estimate Stochastic accelerations, "loose" stations, radio only, $\tilde{\Gamma}_{sat}$. 3) Estimate Stochastic, "loose" stations, radio + optical, $\tilde{\Gamma}_{sat}$. 4) Same as (3), only "tight" stations. 5) Same as (3), only Γ^*_{sat}. 6) Same as (4), only Γ^*_{sat}. Ganymede-relative radial position errors, σ_R vs data arc.

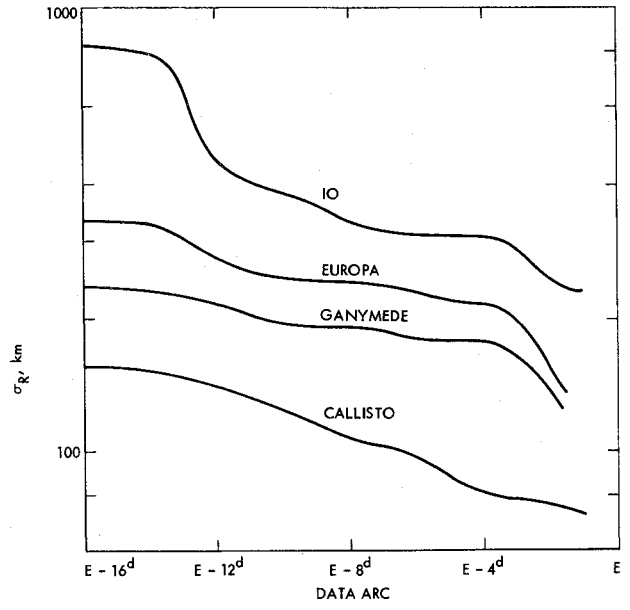

Fig. 10 Satellite-relative radial position error, σ_R vs data arc.

day; 3) only one satellite state is estimated for each case; 4) all four satellite masses are estimated; and 5) the apriori errors in the satellite states are treated two different ways. The first is to use directly the (7x7) covariance generated in the approach phase, designated $\tilde{\Gamma}_{sat}$. The second is to take the radial, downtrack, and out-of-plane position errors from $\tilde{\Gamma}_{sat}$ and to generate a new covariance with the mean motion tightly constrained. Designate this covariance Γ^*_{sat}.

Using these assumptions, a detailed examination of an orbit-phase encounter with Ganymede was made. Figure 9 shows the results of this study. What is displayed here is the radial position error at encounter as a function of the data arc. The downtrack and out-of-plane errors are not displayed

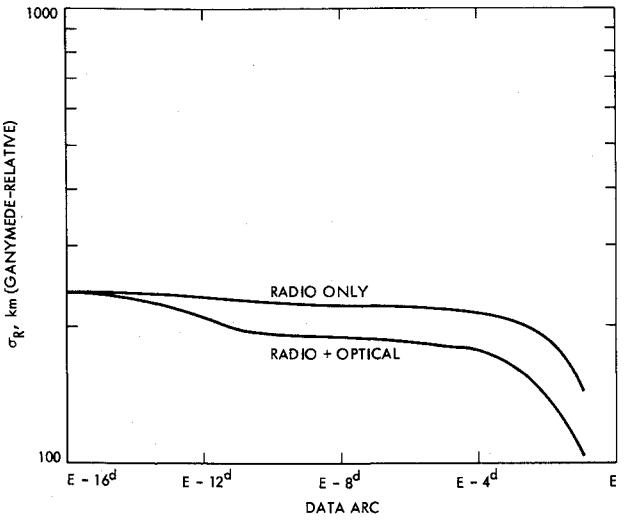

Fig. 11 Ganymede-relative radial position error vs data arc for the best radio and radio + optical cases.

as they are comparatively quite small. Inasmuch as the trajectory bending (and hence the error focusing) is slight, the radial error, σR, is roughly equivalent to the B-plane semimajor axis. Probably the most startling behavior is that exhibited in case 1 where stochastic accelerations are treated as consider parameters. The error growth becomes truly awesome as the data arc approaches encounter. To counteract this behavior, a batch-sequential solution for the stochastic accelerations, using a 2-day batch interval, was attempted. Case 2 details the performance. Certainly the large error growth is contained, but little improvement is noted as the data arc is increased.

The large size of the errors is a direct consequence of the mean motion error contained in $\tilde{\Gamma}_{sat}$. Case 3 displays the anticipated improvement as optical data is added. Case 4 shows, however, that even with optical data added, there exists a reasonably strong sensitivity to the size of the station location errors. Cases 5 and 6 are the same as 3 and 4 only the apriori covariance of satellite state errors used in Γ^*_{sat}, as previously described.

From this it is observed that the strategy that yields the best performance is to estimate the stochastic accelerations and to incorporate the best aprior information about both the satellite state (Γ^*_{sat}) and the station locations. Using this strategy, satellite-relative state errors for all four Galilean satellite inbound encounters were obtained. These results are shown in Fig. 10.

Here the satellite-relative state errors show progressive increases for satellites nearer to Jupiter. This is related to the planet-relative velocity of the satellite. Since the spacecraft orbit intersects the satellite trajectories at angles of roughly 30-60°, an orbit timing error will lead to a satellite-relative radial position error somewhat in proportion to the planet-relative satellite velocity. The major sources or error in these results, as in the approach phase, are the optical biases. The maximum error contribution from J_2, however, is only 1 km.

A final study was made to access whether onboard optical data in orbit phase generated additional satellite-relative state information above and beyond what the radio data coupled with the best satellite state information from the approach phase could provide. The answer to this question appears to be yes, as revealed in Fig. 11. The reason for this is that in spite of the tight planet-relative, satellite and spacecraft state errors, the optical data still provides considerable ability to discern the satellite-relative spacecraft state.

Conclusions

From this study it may be said that: 1) if a near-satellite encounter is desired during approach, radio data alone is insufficient with the present level of planetary and ephemeris

errors; 2) the use of optical data during approach can reduce satellite-relative state errors to the level of about 100 km (SMAA), five days prior to encounter[¶]; 3) The use of appropriately weighted, differenced and conventional radio data can eliminate the effects of stochastic accelerations during the approach phase; 4) the on-board video data is capable of yielding rather precise planet-relative, satellite state information, however, the mean-motion error, using this data type by itself, results in large state errors when mapped [¶]; 5) the elimination of near-periapsis radio data (relative to Jupiter) results in improved state estimation due to a decreased sensitivity to harmonic field errors; 6) with the removal of near-periapsis radio data, both approach and orbit phase results become insensitive to Jupiter harmonic field errors; 7) state estimation is not significantly sensitive to orbit orientation (argument of periapsis); 8) navigation accuracy can be significantly affected by unmodelled accelerations in orbit phase; 9) satellite-relative state errors appear to be a strong function of the satellite encountered; 10) in orbit phase, optical data enhances state estimation beyond what is achieved by radio data alone (including best satellite state information). Areas of future investigation should include outbound satellite encounters and a more comprehensive treatment of on-board video centerfinding and bias errors.

¶These estimates are a significant function of the nature and size of the optical center-finding and bias errors.

References

[1]Uphoff, C., Roberts, P. H., and Friedman, L.D., "Orbit Design Concepts for Jupiter Orbiter Missions," AIAA Paper 74-781, Mechanics and Control of Flight Conference, Anaheim, Calif., 1974.

[2]Anderson, J.D., Null, G.W., and Wong, S.K., "Gravity Results from Pioneer 10 Doppler Data," *Journal of Geophysical Research*, Vol. 79, Sept. 1974, p. 3661.